ELSEVIER

Biophysical Chemistry 112 (2004) 155–163

Biophysical Chemistry

www.elsevier.com/locate/bpc

Quantitative analysis of aggregation in dilute solutions of effectively rigid biomacromolecules via the combination of oscillatory flow birefringence and viscoelasticity measurements: example study of aggregation of bovine fibrinogen in aqueous glycerol, and detection of a large aggregate formed on addition of guanidine hydrochloride

J.W. Miller[1], F.H.M. Nestler[2], J.L. Schrag*

Department of Chemistry and Rheology Research Center, University of Wisconsin, 1101 University Avenue, Madison, WI 53706, United States

Received 18 June 2004; received in revised form 9 July 2004; accepted 9 July 2004
Available online 18 October 2004

Abstract

Oscillatory flow birefringence (OFB) properties have been measured for dilute solutions of bovine fibrinogen in 65–68% aqueous glycerol with the Miller–Schrag Thin Fluid Layer (TFL) apparatus employing either titanium or stainless steel surfaces in contact with the solutions. The shearing frequency range was 1 to 2500 Hz, the concentrations ranged from 4 to 8 mg/ml, and measurement temperatures were 9.9, 10.0, and 15.8 °C. The data showed evidence of significant amounts of aggregation that apparently is caused by the presence of glycerol; contributions from the various aggregates were readily detected since the staggered half-overlap aggregation in this system results in substantial differences in the rotational relaxation times of the various effectively rigid aggregates. The combination of oscillatory flow birefringence and viscoelasticity (VE) data provided sensitive and precise characterization of aggregation in these example systems; all aggregates exhibited the expected positive optical anisotropy. The length of unaggregated fibrinogen in solution was found to be that obtained via electron microscopy. Addition of guanidine hydrochloride to hopefully reduce aggregation did so but also resulted in formation of a very large (2800 to 3500 Å), apparently nearly monodisperse, negatively birefringent aggregate, suggesting that this new species might be formed by lateral aggregation.

Keywords: Fibrinogen; Quantitative analysis of aggregation; Oscillatory flow birefringence

1. Introduction

This article is dedicated to the memory of Professor John D. Ferry, one of the great pioneers in polymer and biopolymer science, with whom we had the privilege and honor to work here at Wisconsin. Sometime late in 1973 John Ferry showed me (John Schrag) new, very dilute solution viscoelasticity data for bovine fibrinogen in a buffered 68% aqueous glycerol solvent. The data was obtained by employing the then new, high precision Birnboim–Schrag multiple-lumped resonator apparatus [1] equipped with a titanium alloy resonator [2]. The frequency dependence observed deviated somewhat from what one expects for a monodisperse system of moderately rigid molecules which John had thought would apply for these solutions. He asked me if I thought that these deviations could be the result of some instrumental error. I reminded him of the high precision of the instrument, and noted that the character of the deviations seemed to suggest contributions from species of various lengths, and thus some type of aggregation. John immediately responded that they had also noticed that the intrinsic viscosity of the solutions

* Corresponding author. Tel.: +1 608 262 3145 or +1 608 263 4450; fax: +1 608 262 0453.
E-mail address: schrag@chem.wisc.edu (J.L. Schrag).
[1] Present address: Pfizer Chemical, retired; 78 Walnut Tree Hill Road, Sandy Hook, CT 06482, USA.
[2] Present address: 331 East 14th St., New York, NY 10003, USA.

0301-4622/$ - see front matter © 2004 Elsevier B.V. All rights reserved.
doi:10.1016/j.bpc.2004.07.015

obtained via capillary viscometry was anomalously high, 33 ml/g, when buffered aqueous solutions (no glycerol) typically showed values around 25 ml/g, also suggesting some aggregation; in addition, removal of the glycerol by dialysis had resulted in a reduction to 24±1 ml/g as expected for native fibrinogen [2,3]. He speculated that when glycerol was present, its lower polarity would favor biomolecular interactions move strongly relative to interaction with solvent, causing aggregates to form (dynamic equilibria) that would have the same staggered half-overlap geometry as for polymerization of fibrinogen, which would lead to a length for an n-mer of $(n+1)/2$ times that of an individual fibrinogen molecule (herein called "monomer"). I pointed out that if this were the case, i.e. that there would be a discrete length distribution for such aggregates, then oscillatory flow birefringence (OFB) would probably provide a powerful means for detecting and quantitatively evaluating the aggregates and their relative concentrations since OFB would be quite sensitive to large aggregates (the intrinsic optical polarizability anisotropy for the n-mer aggregate would effectively be n times that for the "monomer" since no covalent bonds would be formed) and the rotational relaxation time τ for each aggregate would be significantly different (τ is approximately proportional to length cubed). This led us to undertake parallel studies of identical bovine fibrinogen solutions, with the viscoelasticity (VE) measurements being made in Ferry's laboratories by Dr. Norio Nemoto, a postdoctoral associate in his group, or Henry Nestler (then a graduate student), and the oscillatory flow birefringence (OFB) measurements by Jim Miller, then a graduate student in my research group who had recently completed design and construction of a new version (5th generation) of a thin fluid layer oscillatory shear flow birefringence instrument [4–7] (subsequent additional OFB measurements not reported here were carried out by Henry). This collaboration enabled precise determinations of the weakly bound aggregates formed, their relative concentrations, quantitative confirmation of the staggered half-overlap aggregation geometry John had suggested, and led to the publication of the viscoelasticity part of the study in 1977 [2,5]. Combination of the VE and OFB measurements was particularly useful; the VE data reflects the aggregation much differently, so that only if the aggregation information coming from the OFB data analysis and its assumptions are correct will the VE properties be predicted quite precisely [2]. Aggregation in dilute buffered fibrinogen solutions containing glycerol had been suspected for some time since historically various different physical–chemical methods (viscosity, light scattering, electric birefringence, sedimentation, steady flow birefringence; all different in sensitivity to presence of aggregates) had led to substantial variations in apparent fibrinogen length determinations (500 to 860 Å, but assumed no aggregation) while electron micrograph data gave 440±42 Å for the dry molecule [3,8]. The oscillatory flow birefringence part of this collaboration was not published, however, because Jim Miller and Henry Nestler continued the experiments further to see if we could reduce or alter the aggregation by introducing a denaturing agent, guanidine hydrochloride (GHCl). This addition did alter the concentrations of the staggered half-overlap aggregates (positive optical anisotropies), but it also apparently caused the formation of a new, very large, apparently monodisperse aggregate that had negative optical anisotropy, suggesting that a different aggregation geometry (possibly lateral) had now been formed. At this point Henry Nestler graduated, and studies of the new aggregate were left to be completed by future graduate students. Unfortunately, no one was found who had the same expertise and background with fibrinogen. These birefringence studies are described here.

2. Theory

2.1. Oscillatory flow birefringence

Fig. 1a illustrates the overall structure and dimensions assumed here for a fibrinogen molecule [3]; for ease of description, this will be referred to as the "monomer". In this work the monomer is modeled as either a prolate ellipsoid of revolution or as an effectively rigid trinodular rod. Thus for unaggregated monomer solutions sufficiently dilute to avoid significant intermolecular interaction, the ratio of the complex mechano-optic coefficient S^* to its low frequency limiting value S_0 for either of these two models is given by

$$\frac{S^*}{S_0} = \frac{S_M}{S_{M0}}\exp[i(\theta_S - \theta_{S0})] = \frac{1 - i\omega\tau}{1 + (\omega\tau)^2} \quad (1)$$

where the rotational relaxation time τ is that for end-over-end rotation and ω is the angular shearing frequency. (The

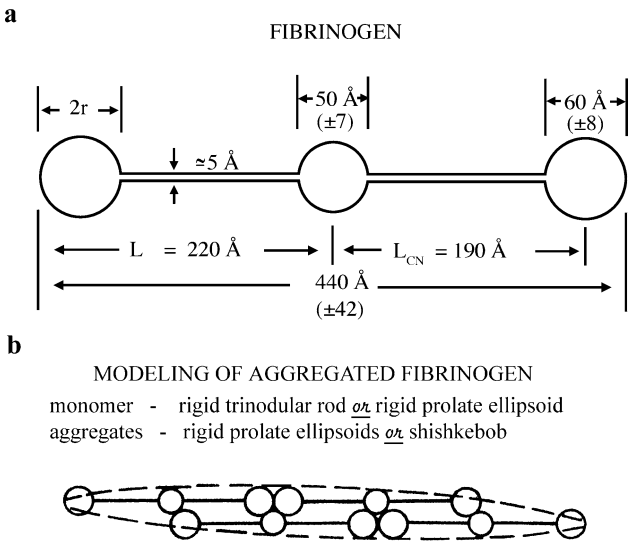

Fig. 1. (a) Overall shape and dimensions of the bovine fibrinogen molecule as determined by electron microscopy [8]. (b) Staggered half-overlap aggregation geometry shown for a tetramer. Equivalent ellipsoid denoted with dashed lines.

mechano-optic coefficient S^* (phaser notation) is defined as [4,6] $S^* \equiv \pm(\Delta n^*/\dot{\gamma}^*) = S_M \exp(i\theta_S) = S' + iS''$, where Δn, the real part of Δn^*, is the difference in indices of refraction in principal directions 1 and 2 and $\dot{\gamma}$, the real part of $\dot{\gamma}^*$, is the sinusoidally time varying shear rate (sign depends on the coordinate system chosen).) For prolate ellipsoids of revolution with axial ratio $p \equiv a/b$ greater than 5, τ can be expressed as [2,9,10]

$$\tau = \frac{8\pi\eta_S a^3}{9kT[2\ln(2p) - 1]} \tag{2}$$

where a and b are the lengths along the major and minor semiaxes, respectively; k is Boltzmann's constant; η_S is the solvent viscosity; and T is absolute temperature. For a rigid trinodular rod with end nodules of equal radius r, Hassager obtained [11]

$$\tau = (2L_{CN})^2\zeta/12kT = \left(2\pi L_{CN}^2\eta_s r\right)/kT \tag{3}$$

where L_{CN} is the distance between end and center nodules (see Fig. 1a) and ζ, the friction coefficient, is assumed to be given by Stokes formula $\zeta = 6\pi\eta_s r$. It should be noted that Eq. (2) assumes full hydrodynamic interaction while Eq. (3) assumes it to be negligible.

2.1.1. Aggregated rigid particle systems

Assume a very dilute solution of effectively rigid macromolecules that is polydisperse due to formation of n-mers (dimers, trimers, etc.; may be either loosely bound or covalently bonded) and that each of these aggregates can be modeled by an appropriate ellipsoid of revolution. Assuming that intermolecular interactions are sufficiently negligible that individual birefringence contributions are simply additive, and that the magnitude of the sinusoidally time varying shear rate is sufficiently low that the extinction angle effectively remains at $\pm 45^\circ$ with respect to the streamline direction throughout the deformation cycle, the Cerf/Thurston treatment yields [12]

$$S^* = S_M \exp(i\theta_S) = \sum_k \frac{A_k}{1 + i\omega\tau_k}, k = 1, \ldots \tag{4}$$

where the subscript k denotes parameters for the k-mer; A_k is given by

$$A_k = \frac{2\pi c_k (g_1 - g_2)_k (p_k^2 - 1)}{15 n_s D_k (p_k^2 + 1)}, k = 1, \ldots \tag{5}$$

with p_k the axial ratio of the equivalent ellipsoid, c_k the concentration (g/cc), $(g_1 - g_2)_k$ the difference in principal polarizabilities in the axis directions, n_S the solvent index of refraction, τ_k the relaxation time for end-over-end rotation, and D_k the rotational diffusion coefficient which is related to τ_k by $D_k = (6\tau_k)^{-1}$. For computational simplicity, Eq. (4) can be written as

$$\frac{S^*}{S_0} = \frac{S_M}{S_{M0}} \exp[i(\theta_S - \theta_{S0})] = \sum_k \frac{(A_k/A_1)[1 - i\omega\tau_1(\tau_k/\tau_1)]}{\frac{1}{1+(\omega\tau_1)^2(\tau_k/\tau_1)^2}} \Big/ \sum_k (A_k/A_1), k = 1, \ldots \tag{6}$$

where subscripts 1 and k denote the monomer and k-mer, respectively. Note that the critical factors are A_k/A_1 and τ_k/τ_1; for prolate ellipsoids with $p > 5$ the τ_k are given by Eq. (2).

For the specific fibrinogen case being considered here, assuming the staggered half-overlap picture suggested by John Ferry (illustrated for tetramer aggregate in Fig. 1b) leads to

$$\frac{L_k}{L_1} = \frac{k+1}{2} \tag{7}$$

where L_k and L_1 are half of the end-to-end lengths for the k-mer and monomer, respectively (L_1=220 Å from Fig. 1a). Assuming all aggregates to be modeled by an equivalent ellipsoid (see Fig. 1b, for example) Eqs. (2) and (7) yield

$$\frac{\tau_k}{\tau_1} = \left(\frac{k+1}{2}\right)^3 \frac{[2\ln(2p_1) - 1]}{[2\ln(2p_k) - 1]} \tag{8}$$

In addition, since the aggregates formed in our case are weakly bound, not covalently bonded (dynamic equilibrium), it is reasonable to assume that the polarizability anisotropy for the k-mer is to a good approximation equal to the sum of the anisotropies for each fibrinogen constituent in the aggregate. Thus $(g_1 - g_2)_k \cong k(g_1 - g_2)_1$ so that, for fibrinogen, assuming the staggered half-overlap picture with equal densities for monomer and aggregates,

$$\frac{A_k}{A_1} = k \frac{c_k}{c_1} \frac{\tau_k}{\tau_1} \frac{p_k^2 - 1}{p_k^2 + 1} \frac{p_1^2 + 1}{p_1^2 - 1} \tag{9}$$

Note that although the (τ_k/τ_1) and (A_k/A_1) ratios contain the axial ratios p_k, since here p_k is generally substantially greater than 5, the sensitivity of these ratios to p_k is quite small. Thus obtaining an accurate value for the semi-minor axis of the kth equivalent ellipsoid is not necessary. For all results shown here the ellipsoid width for the monomer is taken to be 60 Å (see Fig. 1a) and for all staggered half-overlap aggregates, 80 Å (approximate value estimated for half-overlap structure). The (A_k/A_1) and (τ_k/τ_1) ratios obtained for the first eight k-mers are listed in Table 1 for the two models: those subscripted with an E are for the equivalent ellipsoid model for monomer and all k-mers; those subscripted with an S assumed the rigid trinodular rod model for the monomer and a shishkebob model for the aggregates. For the latter shishkebob modelling the calculational details are not given here due to its complexity; see

Table 1
Modeling of aggregated fibrinogen: ratios (τ_k/τ_1) and A_k/A_1 versus k for first eight k-mers for ellipsoid and shishkebob models

k	$(\tau_k/\tau_1)_E$	$(A_k/A_1)_E$	$(\tau_k/\tau_1)_S$[a]	$(A_k/A_1)_S$[a]
1	1	1	1	1
2	3.20	6.46 (c_2/c_1)	2.86	5.74 (c_2/c_1)
3	6.75	20.7 (c_3/c_1)	6.18	18.6 (c_3/c_1)
4	12.1	49.9 (c_4/c_1)	11.5	46.0 (c_4/c_1)
5	19.7	101 (c_5/c_1)	19.3	96.6 (c_5/c_1)
6	29.7	184 (c_6/c_1)	30.2	181 (c_6/c_1)
7	42.6	308 (c_7/c_1)	44.6	312 (c_7/c_1)
8	58.5	485 (c_8/c_1)	63.2	505 (c_8/c_1)

[a] Assuming no hydrodynamic interaction.

Ref. [5] for details. However, note that the trinodular rod and shishkebob model does not include hydrodynamic interaction so that although the molecular geometries might be better represented than with the ellipsoid modeling the omission of hydrodynamic interaction could lead to errors in predicted relaxation times of up to 10% [13,14]. The values obtained for the (τ_k/τ_1) and (A_k/A_1) ratios are nearly the same for both modelings, and both models produced excellent fits to the data.

2.2. Viscoelasticity

For very dilute solutions of effectively rigid macromolecules in which some aggregation is present, the form of the expressions predicting the viscoelastic properties is the same for four different physical models of the macromolecule (ellipsoid, trinodular rod, hinged trinodular rod and cylindrical rod; see Ref. [2] for details). In terms of the complex shear modulus $G^*=G'+iG''=i\omega\eta^*$ (η^* is the complex viscosity coefficient) one has

$$\frac{G'}{c_1}\frac{M_1}{RT} = (\omega\tau_1)^2 \sum_k Z_k \left(\frac{\tau_k}{\tau_1}\right)^2 \frac{m_{Ak}}{1+(\omega\tau_1)^2(\tau_k/\tau_1)^2} \quad (10)$$

and

$$\frac{G''-\omega\eta_s}{c_1}\frac{M_1}{RT} = \omega\tau_1 \sum_k \left(\frac{\tau_k}{\tau_1}\right) \times \left[\frac{m_{Ak}}{1+(\omega\tau_1)^2(\tau_k/\tau_1)^2} + m_{Bk}\right] \quad (11)$$

where m_A and m_B are constants with somewhat different values for the different models [2] and $Z_k=(c_k/c_1)(M_1/M_k)$ where the c's are in g/cc and the M's are the gram molecular weights. From Eq. (11) the low frequency, frequency independent limit of the macromolecular contribution to the steady flow viscosity is

$$\eta_0-\eta_s = \frac{c_1}{M_1}RT\tau_1 \sum_k Z_k\left(\frac{\tau_k}{\tau_1}\right)[m_{Ak}+m_{Bk}] \quad (12)$$

from which

$$\eta_0-\eta_s \simeq B_1 \sum_k \left(\frac{1}{k}\right)\left(\frac{c_k}{c_1}\right)\left(\frac{\tau_k}{\tau_1}\right) \quad (13)$$

since for the four models indicated $m_{Ak}+m_{Bk}$ is roughly equal to one; here $B_1\equiv(c_1/M_1)RT\tau_1$. Similarly from Eq. (4) the low frequency limiting value S_0 of the complex mechano-optic coefficient S^* for the aggregated fibrinogen system assumed to obtain Eq. (9) is given by

$$S_0 = \sum_k A_k = A_1 \sum_k (A_k/A_1) \simeq A_1 \sum_k (k)(c_k/c_1)(\tau_k/\tau_1) \quad (14)$$

since $(\rho_1/\rho_k \simeq 1)$ as is $(\rho_k^2-1)/(\rho_k^2+1)$. Comparing Eqs. (13) and (14) it is clear why the combination of OFB and VE data is desirable for an analysis of this type of aggregating system: for a given k-mer, both the OFB and VE contributions relative to the 1-mer (monomer) are enhanced by the factor (τ_k/τ_1), but the OFB contribution is further enhanced by a factor of k while the VE contribution is *decreased* by the factor $(1/k)$. Thus, for example, for an octamer aggregate the relative magnitude of the ratio of the kth contribution to the monomer contribution is approximately 64 times greater for OFB than for VE. Thus aggregate concentrations that correctly predict the observed properties for both OFB and VE not only give added confidence in the concentration ratios obtained but also validate the various assumptions and approximations employed.

Fig. 2 illustrates the predicted OFB sensitivity to aggregation for the fibrinogen case when each species is represented by an equivalent ellipsoid. Fig. 2a shows log–log plots of the predicted magnitude of S^*/S_0 versus $\omega\tau_1$ where again τ_1 is the relaxation time for the monomer. The lines labeled "monomer" and "octamer" show the predicted curves for monodisperse monomer or octamer solutions, respectively; the curve labeled "monomer+1% octamer/monomer" shows the substantial change relative to the monomer case when an octamer concentration of 1% of that of the monomer is present. The curve "monomer+20% dimer/monomer+3% tetramer/monomer+0.4% octamer/monomer" demonstrates the predicted behavior for an aggregate concentration distribution approximating that seen in our earlier studies in which stainless steel sample cells where used; the presence of stainless steel apparently significantly enhances aggregation, likely due to iron complexation, so all subsequent OFB measurements were made with only titanium alloy or glass in contact with the sample solutions. Fig. 2b shows the predicted phasing of the birefringence $(\theta_S-\theta_{S0})$ versus log $(\omega\tau_1)$, and illustrates the great sensitivity of this quantity to the presence of

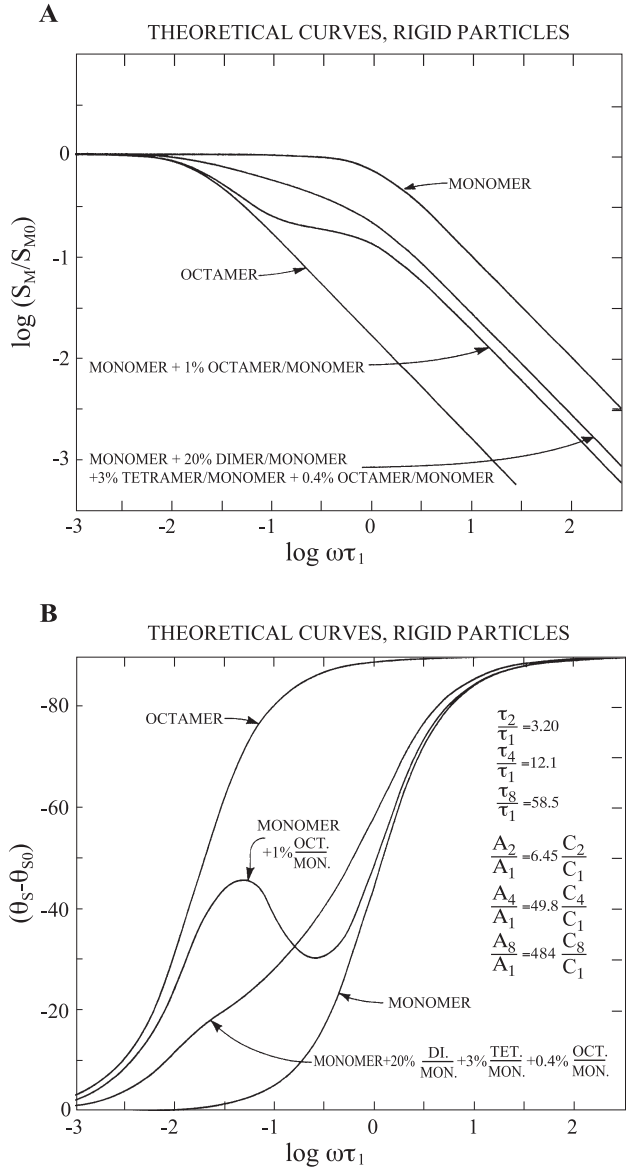

Fig. 2. Logarithmic plots of oscillatory flow birefringence properties in terms of (S_m/S_{m0}) and $(\theta_S-\theta_{S0})$ versus $(\omega\tau_1)$ as predicted for monodisperse and polydisperse distributions of rigid macromolecules modeled as prolate ellipsoids.

aggregates. Fig. 3 illustrates the much lower sensitivity of VE to this aggregation. Fig. 3a illustrates this effect for the same aggregation levels as in Fig. 2; here again the plot is for the ellipsoid modelling case. Note that the shifts and curve shape changes caused by aggregation are rather minimal. Fig. 3b presents predictions for the same distributions but for different modelling; here the fibrinogen monomer is modelled as a rigid trinodular rod (no hydrodynamic interaction) and the other species are modelled by equivalent ellipsoids (full hydrodynamic interaction). Note that the differences in the predictions for these two modellings are insignificant. Fig. 3c plots the VE angle quantity that is the mechanical properties equivalent to $(\theta_S-\theta_{S0})$ (see Fig. 2b) except for the effect of the difference in

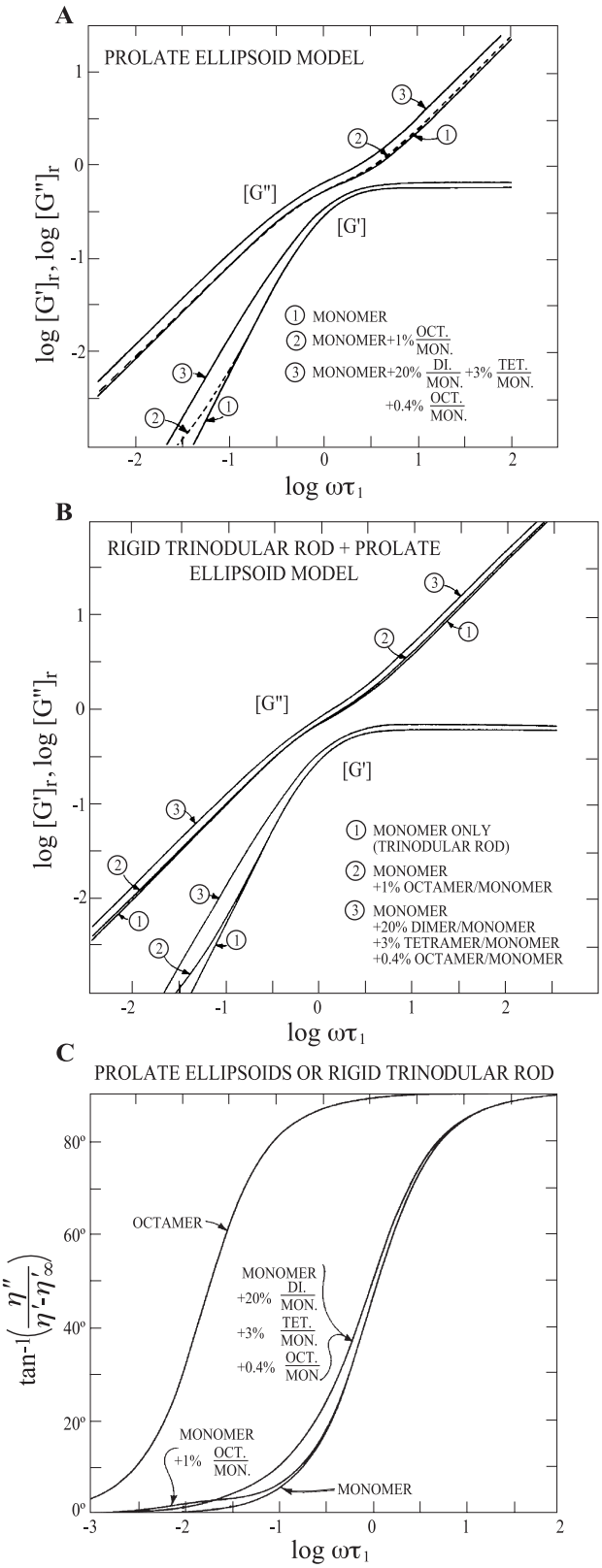

Fig. 3. Logarithmic plots of viscoelastic properties versus $(\omega\tau_1)$ for rigid macromolecules in solution as predicted by two models: (a) all species modeled by equivalent prolate ellipsoids; (b) monomer modeled as a rigid trinodular rod (no hydrodynamic interaction), aggregates modeled as prolate ellipsoids; (c) either modeling, but with predictions in terms of the angle $\tan^{-1}[\eta''/(\eta'-\eta'_\infty)]$.

sensitivity to aggregation for VE relative to OFB. The differences produced by aggregation are clearer in Fig. 3c but are still much less than what is seen in Fig. 2b. In addition, obtaining precise values for the η'_∞ quantity necessary to produce this plot has not been possible to date for any aqueous or aqueous glycerol based solution; the highest measurement frequencies for high precision measurement to date are somewhat less than 10 kHz while frequencies of at least 500 kHz would be required to obtain adequate values for η'_∞.

3. Experimental

3.1. Materials/method

All fibrinogen solutions studied here were prepared by Henry Nestler with assistance from John Ferry after discussions with Professor L. Lorand (Northwestern University). The detailed preparation and purification procedures are contained in Ref. [2]. The buffered solvent contained doubly distilled water and glycerol in weight proportions ranging from 32:68 to 35:65; 68% glycerol is the highest concentration at which denaturation can be avoided according to Allis [15]. As in the VE study [2], glycerol was added to the buffered aqueous solvent to increase its viscosity and hence the relaxation times for the various k-mers to move the incomplete relaxation regime into the experimentally accessible frequency range. The viscosity of the buffered 68% glycerol solvent was 0.172 Poise at 25.0 °C and 0.374 Poise at 10.0 °C [2].

OFB measurements (optical wavelength of 5770 Å) at shearing frequencies from 1 to 2500 Hz were obtained using the Miller–Schrag Thin Fluid Layer (TFL) apparatus[4,5,7] and either a second-generation computerized data acquisition and processing system (DAPS II) or a modified Princeton Applied Research Model 129 A lock-in amplifier. Initially, all instrument surfaces in contact with the solutions were made of stainless steel, but were subsequently replaced by titanium alloy when it became clear that the fibrinogen solutions attacked stainless steel releasing ions which then significantly changed the aggregate distribution. OFB results for both cases are presented in the next section to illustrate this effect.

4. Results and discussion

Figs. 4 and 5 present a comparison of OFB data obtained in the titanium system versus that in a stainless steel system. The dashed curves indicate the phase angle behavior for the fibrinogen monomer assuming that it can be modeled as either a rigid trinodular rod or a prolate ellipsoid with dimensions obtained from electron microscopy (Fig. 1a; p=7.33). The OFB data in both figures exhibit substantial incomplete relaxation effects at much

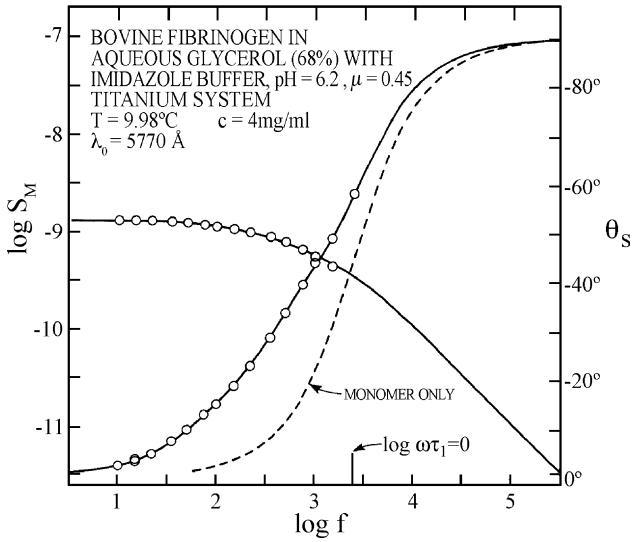

Fig. 4. Plots of log S_M and θ_S versus log frequency for buffered bovine fibrinogen in aqueous 68% glycerol at 10.0 °C, concentration 4.0 mg/ml, in titanium system. Solid curves, best fit predictions for ellipsoid modeling calculated from Eqs. (6), (8) and (9). Dashed curve, θ_S predicted for monomer only.

lower frequencies than the monomer form, indicating that substantial amounts of aggregates are present. The presence of stainless steel in contact with the sample solution appears to enhance aggregation, especially formation of the larger aggregates, a trend seen throughout our preliminary studies. The OFB data were fitted assuming the staggered half-overlap aggregate geometry to apply. First, the relaxation time and (A_k/A_1) ratios were calculated as described earlier (Eqs. (8) and (9)) (see Table 1). Initial estimates for monomer length (440 Å) and species widths (60 Å, monomer; 80 Å, aggregates) as mentioned earlier were used to obtain each axial ratio p_k for the k-mers. Since it is not necessary to know these p_k with precision since Eqs. (8) and (9) are only weak functions of p_k, these initial values were employed throughout the data fitting process. The aggregate/monomer concentration ratios (c_k/c_1) were then determined by fitting the OFB data to Eq. (6) utilizing the (τ_k/τ_1) and (A_k/A_1) ratios of Table 1; fitting was accomplished by Henry Nestler using the NREG nonlinear regression analysis subroutine at the Madison Academic Computing Center. This led to best-fit concentration ratios and monomer relaxation times. Table 2 presents the best-fit concentration ratios for the data of Figs. 4 and 5; ratios are shown for the two models discussed previously. The ratios obtained are quite precise; variation of these by 0.05% led to substantially poorer fits. Likewise, varying the extent of overlap by ±5% from the assumed half-overlap condition led to much poorer fits. The solid curves drawn through the data points in Figs. 4 and 5 are the calculated best-fit OFB predictions (ellipsoid modeling) assuming the concentration ratios of Table 2. If one employs the trinodular rod model for the monomer and the shishkebob model for the aggregates, the best-fit aggregate concentration ratios are

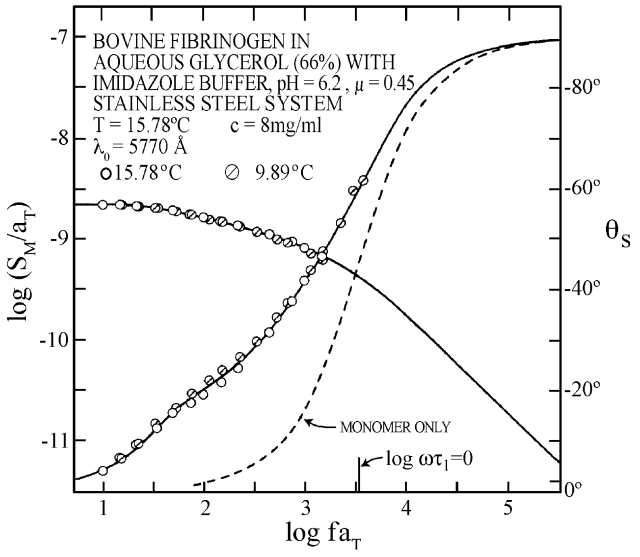

Fig. 5. Plots of log S_M and θ_S versus log reduced frequency (fa_T) (a_T is the time/temperature superposition parameter) for buffered bovine fibrinogen in 66% aqueous glycerol at 9.9 and 15.8 °C, concentration 8.0 mg/ml, in stainless steel system. Solid curves, best fit predictions for ellipsoid model calculated from Eqs. (6), (8) and (9). Dashed curve, θ_S predicted for monomer only.

shifted slightly (see Table 2) as are the τ_1 values. However, the shifts are sufficiently small that the resultant OFB predictions are effectively indistinguishable from the solid lines in the figures.

The best-fit monomer relaxation times, τ_1, that were obtained are: for Fig. 4 (titanium system), $\tau_1=6.45\times10^{-5}$ s at 10.0 °C (ellipsoid model) or 6.43×10^{-5} s at 10.0 °C (shishkebob model); and for Fig. 5 (stainless steel system), $\tau_1=7.15\times10^{-5}$ s at 9.9 °C (ellipsoid model) or 7.05×10^{-5} s at 9.9 °C (shishkebob model). (Note that these values bracket the value obtained in the VE study where for Fig. 2 of Ref. [2] the $\tau_1=6.6\times10^{-5}$ s reduced to 10.0 °C.) Insertion of these values in Eqs. (2) and (3), with $\eta_s=0.374$ Poise yields the following end-to-end lengths for the fibrinogen monomer: in the titanium system, 438 Å (ellipsoid model) or 437 Å (shishkebob model); in the stainless steel system, 458 Å (ellipsoid model) or 455 Å (shishkebob model). (Note again that the shishkebob model calculation does not include hydrodynamic interaction.) These values are certainly reasonable in view of the electron micrograph value of 440±42 Å. If the values of τ_1 determined here are reduced to water at 20 °C to compare with literature results, one obtains $\tau_1=2.2\times10^{-6}$ s (ellipsoid or shishkebob models) in the titanium system or 2.4×10^{-6} s (both models) in the stainless steel system. These are somewhat smaller than the 2.7×10^{-6} s values we reported from the VE data [2]. However, when the VE data of Ref. [2] were analyzed in 1976, we used the aggregate concentration distribution obtained via OFB for a titanium system; at the time we were unaware of the significant alteration of this distribution if the solution was in contact with any stainless steel. The VE measurements were made employing a titanium alloy resonator, but the sample housing was made of stainless steel or aluminum alloy lined with stainless steel. Thus the actual distribution was probably closer to that shown for stainless steel in Table 2. Reanalysis of the VE data employing this distribution substantially improves the agreement between predictions and data compared to what is shown in Fig. 2 of Ref. [2], and leads to a τ_1 value very close to the OFB values. Thus the values of τ_1 from both VE and OFB are significantly smaller than what was previously obtained from rotary diffusion coefficients obtained from steady flow birefringence and electric birefringence ($\tau_1=4.2\times10^{-6}$ s) [2,3]. However, the latter measurements were also made in the presence of glycerol and thus were probably affected by the presence of aggregates. If the aggregation were ignored in our OFB data analysis and the data are fitted to a single relaxation time model (very crude fit), the resultant value for τ_1 is about 4×10^{-6} s when reduced to water at 20 °C, the same as was obtained in the earlier studies [2,3]; this corresponds to an apparent end-to-end length of 530 Å.

If one assumes that aggregation vanishes if glycerol is not present, then our OFB results predict that the intrinsic viscosity would be 24 ml/g in the absence of aggregates, somewhat less than the accepted value of 25 ml/g in aqueous solvents [2,3] but equal to the value found in Ref. [2] after the glycerol was removed by dialysis. Thus it might be possible that a very small amount of aggregation still exists even when no glycerol is present; however, we were unable to evaluate this possibility via OFB measurements since without glycerol present the measurement frequency range required would extend up to at least 10 kHz.

The presence of the aggregates in aqueous glycerol solutions of fibrinogen prevented a direct OFB study of the fibrinogen monomer to further confirm the above results. Thus we decided to extend the OFB studies and look at the effect of addition of guanidine hydrochloride (GHCl) to freshly prepared solutions of bovine fibrinogen in buffered 65% or 68% aqueous glycerol in an attempt to eliminate the aggregates; all measurements were made in the titanium system. The results obtained are illustrated in Fig. 6. Note that data for five different solutions are

Table 2
Species concentration ratios from OFB: bovine fibrinogen in aqueous glycerol with imidazole buffer, pH=6.2, μ=0.45

Concentration rations	Stainless steel cell (c=8 mg/ml)		Titanium cell (c=4 mg/ml)	
	Ellipsoids	Shishkebobs	Ellipsoids	Shishkebobs
(c_2/c_1)	18.1%	16.8%	13.5%	11.7%
(c_3/c_1)	3.65%	6.45%	6.46%	8.31%
(c_4/c_1)	2.29%	1.36%	0	0
(c_5/c_1)	0	0.65%	0.17%	0.26%
(c_6/c_1)	0	0	0.4%	0.40%
(c_7/c_1)	0	0	0	0
(c_8/c_1)	0.49%	0.45%	0	0

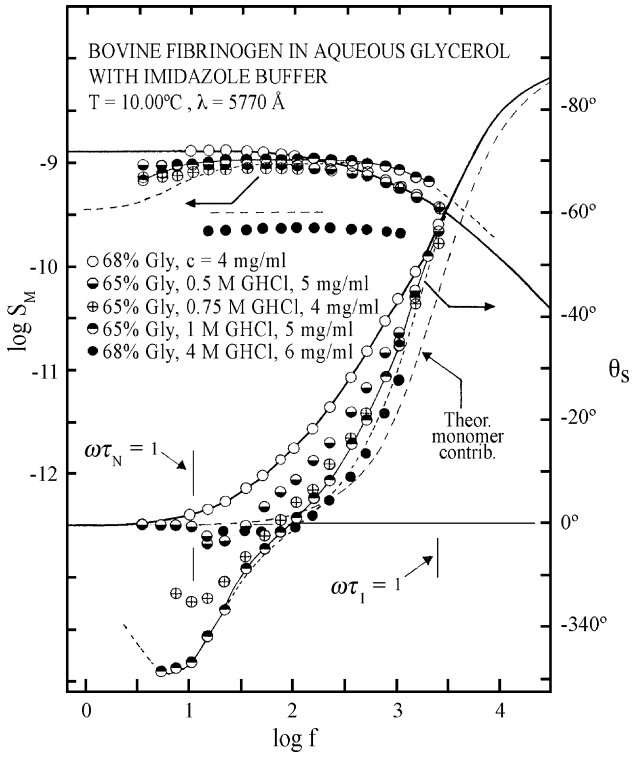

Fig. 6. Plots of log S_M and θ_S versus log f for five buffered bovine fibrinogen solutions; various amounts of GHCl added to four solutions as shown. Solid heavy lines, best-fit theoretical predictions (ellipsoid model) for solution with no GHCl added. Solid thin line not theoretical prediction, but drawn for clarity, connects data points for 1 M GHCl case. Thin line, long dashes: theoretical predictions for two component system with one positive, one negative birefringence contribution with (τ_P/τ_N)=0.0064 and very low frequency component birefringence magnitude ratio=0.65.

shown, and that the fibrinogen concentration varies somewhat (from 4 to 6 mg/ml); the heavy solid lines are the theoretical best fit to the 4 mg/ml, 68% glycerol case (same solution as in Fig. 4), while the light long dashed lines correspond to the predicted monomer contribution to S_M and θ_S for this same solution. Additional data points are shown for four similar solutions containing 0.5, 0.75, 1.0 or 4 M GHCl; the results for these four cases are rather astonishing. Clearly the addition of GHCl has a pronounced effect on the measured OFB properties, and its effect is not simple. First, the concentrations of the aggregates with positive optical anisotropies (those seen with no GHCl added) that have been described to this point are clearly reduced as the concentration of GHCl is increased. However, for all four solutions containing GHCl the θ_S curves drop below 0° at frequencies below about 100 Hz. Also, S_M decreases again with decreasing frequency below about 10 Hz. This strongly suggests that a very large, elongated new aggregate has been formed which has a negative intrinsic optical anisotropy. This negative birefringence contribution increases in magnitude with increasing GHCl concentration up to at least 1.0 M. Apparently this negative birefringence is being produced by a very large, elongated and fairly monodisperse laterally aggregated structure (aggregation direction appears to be perpendicular to the long axis of fibrinogen). Although the addition of GHCl does result in reduction in concentration of the aggregates originally seen, the 1 M GHCl case still shows a significant amount of dimer to be present. To obtain some idea of the size and intrinsic optical anisotropy of this new aggregate the data for the 1 M GHCl solution has been fitted to a theoretical curve (light, narrow dashed lines); a light, solid line (not a theoretical prediction) has also been drawn through these data points to help visualize the experimental curve shapes for this case. The theoretical curve drawn for this case is for a simplified picture of the solution to evaluate the species generating the negative birefringence; since the positive birefringence comes primarily from the monomer and dimer species and is of little interest here, their contribution is approximated by a positive contribution assumed to have a relaxation time $\tau_P=9\times10^{-5}$ s, approximately the average of τ_1 and τ_2. The negative birefringence contribution is assumed to be that from a monodisperse species with relaxation time τ_N. The theoretical curve drawn (narrow dashes) corresponds to the case where $\tau_N \simeq 1.5\times10^{-2}$ s and the magnitude ratio of negative birefringence to positive birefringence at very low frequency (below 1 Hz) is 0.65. If one assumes that the new species can also be represented geometrically by an ellipsoid of revolution, the end-to-end length of this very large structure is somewhere between 2800 and 3500 Å if the axial ratio p is between 10 and 100. The excellent fit of the theoretical curve at frequencies below 75 Hz indicates an essentially monodisperse size distribution for the new aggregate and that it is effectively rigid; the rather approximate fit shown between 75 and 1000 Hz is a result of approximating the positive birefringence term as that coming from a single species. Finally, the data for the 4 M GHCl case suggests that the positive birefringence part is now caused primarily by the monomer form of fibrinogen, but a very small amount of dimer is still present. The concentration of the new aggregate species exhibiting negative birefringence is now also quite small, but a detectable amount is still present and its length apparently has not been altered significantly. Note that the origin of this negative birefringence does not correspond to that of the negative birefringence reported by Haschemeyer and Tinoco [16] and by Haschemeyer [17]; the negative birefringence seen by them in the pH region of 4 to 5 was a result of a transverse permanent dipole moment being formed caused by the titration of two α-amino groups. Here the negative birefringence is the result of a negative intrinsic optical polarizability, which seems to us to suggest that extensive lateral aggregation has taken place, possibly involving of the order of 40 to 50 fibrinogen "monomers." Extensive aggregation has very recently been seen in some protein solutions to which another denaturing agent, urea, has been added; these species were detected in light scattering experiments of

Chow et al. [18] here at Wisconsin. (We also attempted to reduce aggregation in our fibrinogen solutions by the addition of urea. Again, huge aggregates were formed, but were so large that they precipitated out of solution.) Large aggregates apparently have also been seen by various techniques in early stages of conversion of fibrinogen to fibrin (M.W. Mosesson, The Blood Research Institute, Milwaukee WI, (2004), private communication).

5. Conclusions

The combination of oscillatory flow birefringence and viscoelasticity measurements can provide a sensitive and precise characterization of aggregation in macromolecular solutions if the macromolecules are effectively fairly rigid and the aggregates are significantly different in length. For the example bovine fibrinogen solutions studied here the addition of glycerol produced significant reversible aggregation with the staggered half-overlap geometry suggested by John Ferry; changes in pH and ionic strength, and addition of very low levels of metal (probably iron) ion, can substantially alter the distribution function for these positively birefringent species. The end-to-end length obtained for a single fibrinogen (monomer) from the birefringence data is the same as that obtained via electron microscopy for the dried molecule. Staggered half-overlap aggregation beyond the 8-mer has not been detected. However, addition of GHCl resulted in formation of a new, very large, apparently monodisperse, negatively birefringent aggregate, where the aggregation appears to be transverse and probably involves at least 40 fibrinogen molecules (end-to-end length is probably between 2800 and 3500 Å).

Acknowledgements

This work was supported in part by grant numbers DMR72-03017 and DMR76-81715 from the National Science Foundation, a grant from the donors of the Petroleum Research Fund administered by the American Chemical Society, and grant GM21652 from the National Institutes of Health. We are indebted to Professors L. Lorand, R.B. Bird, and C.F. Curtiss for valuable discussions.

References

[1] J.L. Schrag, R.M. Johnson, Application of the Birnboim multiple lumped resonator principle to viscoelastic measurements of dilute macromolecular solutions, Rev. Sci. Instrum. 42 (1971) 224–232.
[2] N. Nemoto, F.H.M. Nestler, J.L. Schrag, J.D. Ferry, Infinite dilution viscoelastic properties of fibrinogen and intermediate fibrin polymer, Biopolymers 16 (1977) 1957–1969.
[3] R.F. Doolittle, Structural aspects of the fibrinogen to fibrin conversion, Adv. Protein Chem. 27 (1973) 1–109.
[4] J.W. Miller, J.L. Schrag, Oscillatory flow birefringence of low molecular weight polystyrene solutions—high frequency behavior, Macromolecules 8 (1975) 361–364.
[5] J.W. Miller, Oscillatory Flow Birefringence Studies of Synthetic and Biological Macromolecules in Solution, PhD thesis in Chemistry, University of Wisconsin, Madison (1979).
[6] G.B. Thurston, J.L. Schrag, Oscillatory flow birefringence of polymer molecules in dilute solutions, J. Chem. Phys. 45 (1966) 3373–3380.
[7] J.L. Schrag, Deviation of velocity gradient profiles from the 'Gap Loading' and 'Surface Loading' limits in dynamic simple shear experiments, Trans. Soc. Rheol. 21 (1977) 399–413.
[8] W. Krakow, G. Endres, B. Siegel, H. Scheraga, An electron microscopic investigation of the polymerization of bovine fibrinogen monomer, J. Mol. Biol. 71 (1972) 95–103.
[9] F. Perrin, Brownian movement of an ellipsoid: I. Dielectric dispersion of an ellipsoidal molecule, J. Phys. Radium, Ser. 7 5 (1934) 497–511.
[10] R. Cerf, Physique macromoleculaire. Sur l'action d'ondes transversales de fréquence ultra-sonique dans les solutions de hauts polymères rigides, C. R. Acad. Sci. 234 (1952) 1549–1551.
[11] O. Hassager, Kinetic theory and rheology of bead—rod models for macromolecular solutions: II. Linear unsteady flow properties, J. Chem. Phys. 60 (1974) 4001–4008.
[12] R. Cerf, G.B. Thurston, Sur la Birefringence Dynamique en Champ Periodique des Solutions Macromoleculaires en Relation avec Leurs Proprietes Visco-Eleastiques, J. Chim. Phys. 61 (1964) 1457–1462.
[13] C.F. Curtiss, R.B. Bird, O. Hassager, Kinetic theory and rheology of macromolecular solutions, Adv. Chem. Phys. 35 (1976) 31–117.
[14] R.B. Bird, O. Hassager, R.C. Armstrong, C.F. Curtiss, Dynamics of Polymeric Liquids, vol. II Kinetic Theory, Wiley, New York, 1977.
[15] J.W. Allis, Viscoelastic Properties of Some Biological Macromolecules in Dilute Solutions, PhD thesis in Chemistry, University of Wisconsin, Madison (1965).
[16] A.E.V. Haschemeyer, I. Tinoco Jr., Charge distribution of fibrinogen as determined by transient electric birefringence studies, Biochemistry 1 (1962) 996–1004.
[17] A.E.V. Haschemeyer, A polar intermediate in the conversion of fibrinogen to fibrin monomer, Biochemistry 2 (1963) 851–858.
[18] C. Chow, R.M. Murphy, S. Cavagnero, Structural Characterization of Apomyoglobin Aggregates in Aqueous Buffer and Urea Solution by Static and Dynamic Light Scattering, Biophys. J. (submitted for publication).